J Polym Res (2017) 24: 50
DOI 10.1007/s10965-017-1203-x

ORIGINAL PAPER

Nitrocellulose-based hybrid materials with T7-POSS as a modifier: effective reinforcement for thermal stability, combustion safety, and mechanical properties

Xiaomei Yang[1] · Yuanyuan Li[1] · Yiliang Wang[1] · Yunguo Yang[1] · Jianwei Hao[1]

Received: 21 September 2016 / Accepted: 13 February 2017 / Published online: 9 March 2017

Abstract Novel nitrocellulose (NC)-based hybrid materials with self-synthesized heptaphenyltricycloheptasiloxane trihydroxy silanol (T_7-POSS) as a modifier were prepared using a "one-step" chemical cross-linking process. To comprehensively demonstrate the superiority of the modifier, hybrid materials with different contents of T_7-POSS were assessed. The gel content was measured, and the chemical structure and composition of the T_7-POSS-NC hybrid materials were characterized by attenuated total reflection Fourier transform infrared spectroscopy (ATR-FTIR) and X-ray photoelectron spectroscopy (XPS). Thermogravimetric analysis (TGA) results showed that the thermal stability of the T_7-POSS-NC hybrid materials increased with the T_7-POSS content. Typically, when 12.3 wt.% T_7-POSS was incorporated into the NC, the decomposition temperature based on 50% weight loss ($T_{50\%}$) was delayed from 183.3 °C to 243.5 °C, the maximum weight loss rate (WLR_{max}) decreased markedly from 432.9%/min to 1.3%/min, and the char residues increased from 1.4% to 26.0%. The scanning electron microscopy (SEM) results of the char residues indicated that the introduction of T_7-POSS led to the formation of a sufficient and compact char layer. Notably, the incorporation of T_7-POSS improved not only the combustion safety according to micro-scale combustion calorimeter (MCC) results but also the mechanical properties due to the formation of cross-linking networks and the good distribution of T_7-POSS particles, which was confirmed by SEM and energy-dispersive spectroscopy (EDS).

✉ Jianwei Hao
hjw@bit.edu.cn

[1] National Engineering Technology Research Center of Flame Retardant Materials, School of Materials Science and Engineering, Beijing Institute of Technology, Beijing 100081, People's Republic of China

Keywords Nitrocellulose · POSS · Cross-linking · Combustion safety · Thermal stability

Introduction

Nitrocellulose (NC) with low nitrogen content, produced from the esterification of natural cellulose through the addition of nitric acid, has been used in different applications [1]. For example, it forms a tough thermoplastic film on photographic film, and it has also been applied in the coating, printing ink, adhesive, and artificial leather fields [2, 3]. Unfortunately, the poor thermal stability and the rapid burning of NC (the rate of combustion of a NC film is approximately 15 times faster than that of wood [4]) limit its use in many desirable applications. As previously reported, NC with 12.1 ~ 12.3% nitrogen content showed a very steep loss in weight, amounting to approximately 99% of the original weight [5], far more than cellulose, which puts its applications in jeopardy. The poor mechanical properties of NC also restrict its widespread use [6, 7].

Some studies have reported various strategies to improve the thermal stability of NC with high nitrogen content, including adding different stabilizers [8], mixing in α-Fe_2O_3 nanoparticles [9] or graphene oxide water solution [10], and washing with industrial water and inorganic salts [11]. However, to the best of our knowledge, there has been no report in the open literature on improving both the thermal stability and combustion safety of NC with low nitrogen content.

Hybrid materials, including both blends in which inorganic phases are physically dispersed in organic matrices, and networks in which the inorganic and organic components are linked through strong chemical bonding, have attracted attention for their potential in combining excellent thermal stability

Scheme 1 Synthetic route of T_7-POSS

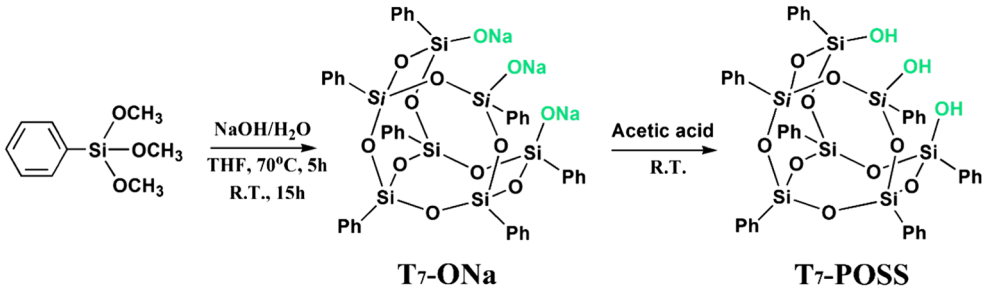

[12, 13] and mechanical properties [14–16]. Recently, polyhedral oligomeric silsesquioxane (POSS), which has an organic-inorganic structure, was introduced into polymer matrices to construct POSS-containing hybrid materials. For example, Bershtein V. synthesized a series of CER/ECH-POSS hybrid materials with varying POSS contents [17].

Many methods have been used to prepare cross-linked hybrid materials; these methods include the sol-gel process, high-energy radiation cross-linking, and chemical cross-linking [18–20]. Among these methods, chemical cross-linking is one of the most effective method because it is not very time- or energy- consuming, and can be performed without radiation.

Thus, in this work, to increase the thermal stability and improve the combustion safety as well as the mechanical properties of NC, heptaphenyltricycloheptasiloxane trihydroxy silanol (T_7-POSS), which has three -OH groups in each POSS unit, was synthesized and used as a modifier to prepare novel cross-linked T_7-POSS-NC hybrid materials via a "one-step" chemical method. Then, the thermal decomposition characteristics, combustion safety and mechanical properties of the samples were systematically evaluated.

Experimental

Materials

NC (nitrogen content ~11.91 wt.%) was kindly provided by Baoding BaoFeng Nitrocellulose Co., Ltd. (Hebei, China). All NC samples were pre-treated in a freeze dryer at −80 °C for 48 h to remove residual water; the samples were then stored in a desiccator before use. Phenyltrimethoxysilane, 97% (Alfa Aesar) was used without further treatment. Dibutyltin dilaurate (DBTL) as a catalyst and isophorone diisocyanate (IPDI) as a cross-linker were purchased from Alfa Aesar. Tetrahydrofuran (THF) and N, N-dimethylformamide (DMF) were further purified by distillation over CaH_2 and stored in a sealed vessel with a molecular sieve of 4 A. All other reagents were obtained from Beijing Chemical Works and used as received.

Preparation

Synthesis of T_7-POSS

Heptaphenyltricycloheptasiloxane trisodium silanolate (T_7-ONa) was synthesized according to the literature [21]. Typically, phenyltrimethoxysilane (10.0 g, 0.05 mol), deionized water (1.15 g, 0.06 mol), THF (80 mL) and sodium hydroxide (0.85 g, 0.02 mol) were charged into a three-necked flask equipped with a reflux condenser and a magnetic stirrer. The mixture was refluxed in an oil bath at 70 °C for 5 h and then cooled to room temperature for an additional 15 h with vigorous stirring. After filtration, the precipitate was collected and washed with THF three times. The resulting white powder was dried in vacuum at 50 °C for 24 h to obtain 6.98 g of the products with a yield of 97%.

T_7-POSS was obtained as follows [22]: 5 g T_7-ONa and 50 mL trichloromethane were added into a separatory funnel, and several droplets of acetic acid were added. After vigorous shaking and washing with deionized water more than three times, the organic phase was precipitated into 400 mL hexane to obtain

Scheme 2 Synthetic route of T_7-POSS-NC hybrid materials

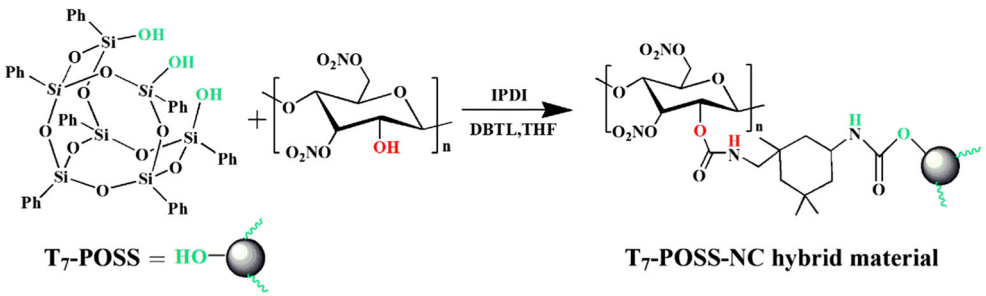

Table 1 Preparation of NC control and T_7-POSS-NC hybrid materials

Samples	NC (g)	IPDI (g)	T_7-POSS (g)	T_7-POSS (wt.%)
NC control	6	0	0	0
4.5 wt.% T_7-POSS-NC	6	0.4	0.3	4.5
8.6 wt.% T_7-POSS-NC	6	0.4	0.6	8.6
12.3 wt.% T_7-POSS-NC	6	0.4	0.9	12.3

white powders with a yield of 89%. The synthetic route of T_7-POSS is shown in Scheme 1.

Preparation of T_7-POSS-NC hybrid materials

The synthetic route of the T_7-POSS-NC hybrid materials is shown in Scheme 2. The general preparation procedures of the T_7-POSS-NC hybrid materials are as follows. NC (6 g) was charged into a beaker with anhydrous DMF (20 mL) and stirred at ambient temperature for 1 h by mechanical stirrer. After the formation of a NC homogeneous solution, an anhydrous DMF solution (10 mL) of T_7-POSS (with different contents) and IPDI (0.4 g) were added into the flask with vigorous stirring for 20 min, and then the bubbles were removed by ultrasonication for approximately 10 min. Subsequently, the mixture was poured into a PTFE casting mold with dimensions of 100 mm × 100 mm to obtain hybrid films of ~1 mm thickness at specific conditions (dried for 2 d at room temperature and for 2 h at 70 °C in an oven). Finally, the films were put in a vacuum for 48 h to remove any residual solvent. From this process, a series of T_7-POSS-NC hybrid materials were obtained, following the detailed preparation presented in Table 1.

Characterization methods

Structural characterization

T_7-POSS Fourier transform infrared spectroscopy (FTIR) was performed in the range of 4000 ~ 400 cm^{-1} with a Tensor-27 (Bruker) using the KBr disk method at room temperature. ^{29}Si nuclear magnetic resonance (^{29}Si NMR) spectra were measured at 400 MHz using an AV400 (Bruker) in $CDCl_3$ at 25 °C, and tetramethylsilane (TMS) was used as an internal standard. An electrospray mass spectrometer (ES-MS) was applied with UPLC-Q-Tof-MS (Waters) using CH_3OH as the solvent.

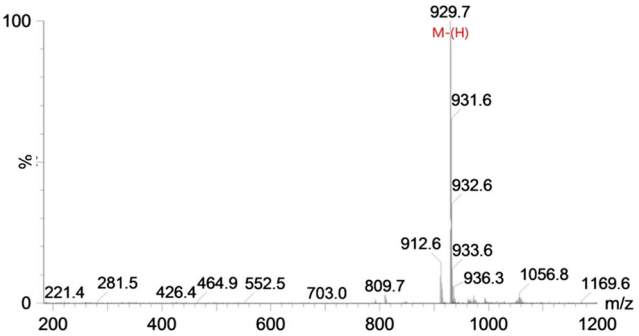

Fig. 2 ES-MS spectrum of T_7-POSS

T_7-POSS-NC hybrid materials The samples were cut into strips, weighed (W_1), and then immersed in tetrahydrofuran (THF) in stoppered bottles for 72 h (solvent was replaced every 24 h) to ensure that the uncross-linked components were extracted completely. The swelled samples were then removed and dried under vacuum (60 °C) to constant weights (W_2). The gel content was calculated according to Eq. (1) [23]:

$$\text{Gel content} = \frac{W_2}{W_1} \times 100\% \quad (1)$$

Each sample was tested at least three times. The gel content efficiency was calculated according to Eq. (2):

$$\text{Gel content efficiency} = \frac{\text{Gel content}}{\text{Weight percentage of T7-POSS}} \times 100\% \quad (2)$$

Attenuated total reflection Fourier transform infrared (ATR-FTIR) spectra were collected in the range of

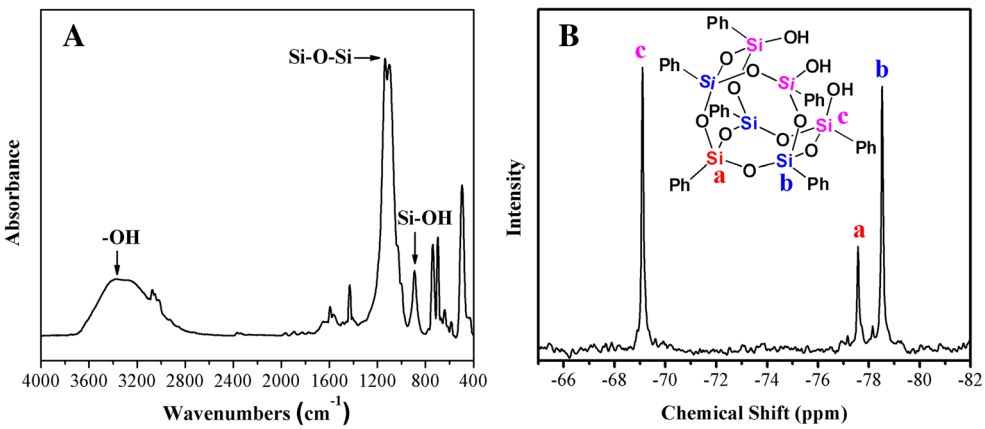

Fig. 1 (**a**) FTIR and (**b**) ^{29}Si NMR spectra of T_7-POSS

Table 2 Gel content and gel content efficiency of NC control and T_7-POSS-NC hybrid materials

Samples	Gel content (%)	Gel content efficiency [a]
NC control	0	-
4.5 wt.% T_7-POSS-NC	40.6 ± 2.4	9.0
8.6 wt.% T_7-POSS-NC	60.7 ± 3.1	7.1
12.3 wt.% T_7-POSS-NC	65.5 ± 3.8	5.3

[a] : *T_7-POSS contribution per unit mass to the gel content*

4000 ~ 400 cm^{-1} using a Nicolet 6700 FTIR spectrometer at room temperature; the spectra were collected at 32 scans with a spectral resolution of 4 cm^{-1}. The elemental compositions of the surfaces were determined by X-ray photoelectron spectroscopy (XPS) (PHI Quantera II SXM) at 25 W under a vacuum environment less than 2.6×10^{-6} Pa using an Al K_α X-ray source. The pass energy is 26.0 eV, and the step length is 1 eV. The weight content of Si (Si %) for each sample was calculated according to Eq. (3):

$$Si\% = \frac{C_A(Si) \times M(Si)}{C_A(C)M(C) + C_A(O)M(O) + C_A(N)M(N) + C_A(Si)M(Si)} \times 100\% \quad (3)$$

where C_A (C), C_A (O), C_A (N) and C_A (Si) represent the atomic concentrations (C_A) of the C, N, O and Si elements on the surface of the T_7-POSS-NC hybrid materials, respectively, and M(C), M (O), M (N) and M (Si) are their relative atomic masses (M).

Thermal stability

Thermogravimetric analysis (TGA) was performed using a TG209 (NETZSCH) with a continuous flow of a N_2 atmosphere. Samples (5 ~ 10 mg) were heated from 50 °C to 500 °C at a rate of 10 °C/min. The following parameters were determined: initial decomposition temperature based on 5% weight loss ($T_{5\%}$), middle decomposition temperature based on 50% weight loss ($T_{50\%}$), maximum weight loss rate (WLR_{max}) and char residues under 500 °C ($CR_{500\ °C}$).

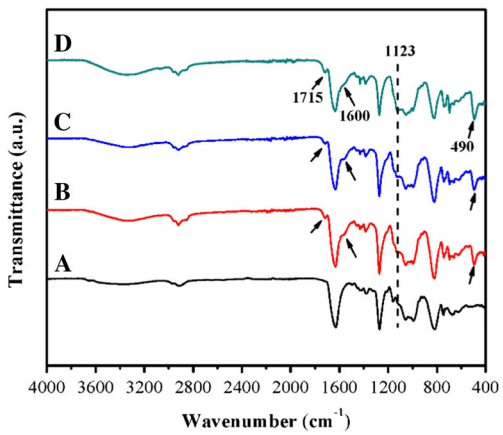

Fig. 3 ATR-FTIR spectra of NC control (**A**), 4.5 wt.% T_7-POSS-NC (**B**), 8.6 wt.% T_7-POSS-NC (**C**) and 12.3 wt.% T_7-POSS-NC (D)

Combustion safety

The combustion safety was evaluated using a micro-scale combustion calorimeter (MCC) (FAA-PCFC) according to ASTM D7309. The samples were cut into strips (~ 2 mg) and heated from 135 °C to 180 °C at a constant heating rate of 0.5 °C/s in a pyrolysis chamber under a nitrogen gas stream (80 cm^3/min). The pyrolysis products were purged from the pyrolysis chamber by the nitrogen gas stream and then mixed with an oxygen gas stream (20 cm^3/min) prior to entering a 900 °C combustion furnace for the no flaming combustion (oxidation).

Mechanical properties

Rectangular tensile bars measuring 50 mm × 10 mm × 0.1 mm were obtained using a fresh razor blade. Uniaxial tensile tests (INSTRON1185) were carried out at 25 °C with a crosshead speed of 5 mm/min. The modulus of each sample was determined by linearly fitting the elastic portion of the stress-strain curve, and the results were the averages of 5 measurements.

Morphology and distribution

The morphology of the char residues after TGA testing was determined by scanning electron microscopy (SEM) (Hitachi S-4700). The samples were quenched and fractured in liquid nitrogen in preparation for the examination of the T_7-POSS distribution by SEM and energy-dispersive spectroscopy (EDS). Prior to the imaging, the surfaces of the samples were sputter-coated with gold.

Table 3 Elemental compositions of the surface for NC control and T_7-POSS-NC hybrid materials

Samples	Atomic conc. (%)				Weight content of Si (%)
	C	N	O	Si	
NC control	70.12	1.73	28.15	0	0
4.5 wt.% T_7-POSS-NC	87.07	2.63	9.05	1.25	2.77
8.6 wt.% T_7-POSS-NC	71.65	5.41	20.26	2.69	5.64
12.3 wt.% T_7-POSS-NC	63.73	4.34	28.93	3.00	6.12

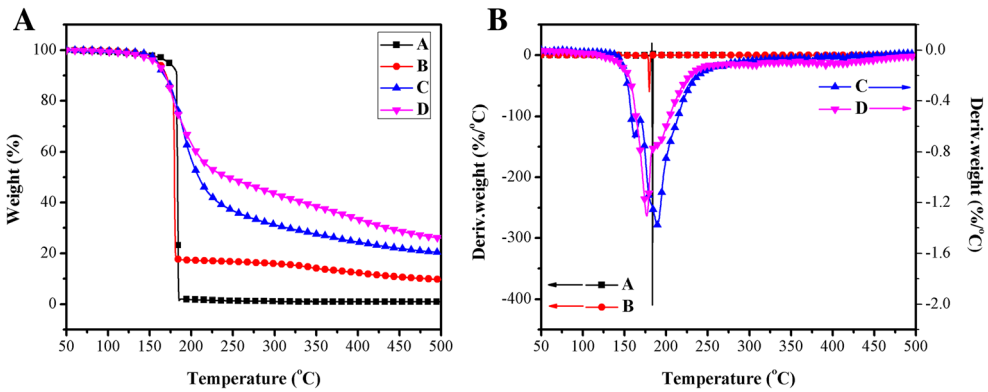

Fig. 4 TGA (a) and DTG (b) curves of NC control (**A**), 4.5 wt.% T_7-POSS-NC (**B**), 8.6 wt.% T_7-POSS-NC (**C**) and 12.3 wt.% T_7-POSS-NC (**D**)

Results and discussion

Structure of T_7-POSS

The FTIR spectrum of synthesized T_7-POSS is presented in Fig. 1(a). The absorption peaks at 3073 cm^{-1}, 1768–1964 cm^{-1}, 1591 cm^{-1} and 1432 cm^{-1} are attributed to Si-Ph vibrations, and the absorption peaks at 891 cm^{-1} and 3234 cm^{-1} are attributed to the stretching vibrations of Si-OH. Peaks at 1134–1101 cm^{-1} that correspond to Si-O-Si vibrations also appear in the spectrum, which indicates that the reaction occurred. The ^{29} Si NMR spectrum of T_7-POSS in $CDCl_3$ (ppm) is presented in Fig. 1(b). The signal at −77 ppm is assigned to Si-O-Si-O-Si-OH (peak a), the signal appearing at −78 ppm corresponds to Si-O-Si-OH (peak b) and the signal at −69 ppm is attributed to Si-OH (peak c). ES-MS was set to record the m/z of the micro molecules, and a significant molecular ion peak at m/z = 929.7 (Fig. 2) was obtained for T_7-POSS. All of these data indicate that the T_7-POSS was successfully synthesized.

Structure and composition of NC control and T_7-POSS-NC hybrid materials

Gel content of T_7-POSS-NC hybrid materials

The gel content represents the weight fraction of the polymers participating in the cross-linked network. It can be seen that the gel content increases with the increasing T_7-POSS content, suggesting that T_7-POSS can promote the formation of a cross-linked structure. To analyze the T_7-POSS contribution per unit mass to the gel content, the gel content efficiency is evaluated, and the related data are shown in Table 2. The degree of increase of gel content and the gel content efficiency decrease gradually. This result may be attributed to the near-saturation of cross-linked point under the circumstance of the same IPDI contents. That is, additional unreacted T_7-POSS particles will be in the presence of the physical blending state.

Table 4 TGA and DTG data of NC control and T_7-POSS-NC hybrid materials

Samples	$T_{5\%}$ (°C)	$T_{50\%}$ (°C)	WLR_{max} (%/min)	$CR_{500\,°C}$ (%)
NC control	172.9	183.3	432.9	1.4
4.5 wt.% T_7-POSS-NC	160.6	179.6	59.5	9.7
8.6 wt.% T_7-POSS-NC	159.5	208.9	1.4	20.3
12.3 wt.% T_7-POSS-NC	158.3	243.5	1.3	26.0

Structure of NC control and T_7-POSS-NC hybrid materials

ATR-FTIR spectral analysis was conducted to characterize the structures of NC control and T_7-POSS-NC hybrid materials (see Fig. 3). It should be noted that 4.5 wt.% T_7-POSS-NC, 8.6 wt.% T_7-POSS-NC and 12.3 wt.% T_7-POSS-NC here have had the unreacted substances extracted. For the all samples, the two characteristic peaks at 1635 cm^{-1} and 1285 cm^{-1} are attributed to -NO_2 asymmetric and symmetric stretching vibrations, respectively, whereas the peak at 824 cm^{-1} is related to the -ONO_2 vibrations of NC. 4.5 wt.% T_7-POSS-NC, 8.6 wt.% T_7-POSS-NC and 12.3 wt.% T_7-POSS-NC exhibit typical transmittance at 1715 cm^{-1}, which is attributed to the C = O of the T_7-POSS-NC hybrid materials. Moreover, new peaks near 1600 cm^{-1} are assigned to the urethane bond, suggesting that chemical reactions occurred between the hydroxyl groups (−OH) in T_7-POSS and NC and the isocyanate group (−NCO) in IPDI. The successful cross-linking of T_7-POSS onto NC can be further confirmed by the appearance of dominant Si-O-Si stretching vibrations at 1123 cm^{-1} and 490 cm^{-1} [24, 25].

Composition of NC control and T_7-POSS-NC hybrid materials

To further prove the successful cross-linking reaction, XPS was used to detect the atomic concentrations of the C, N, O and Si elements on the surface of T_7-POSS-NC hybrid materials with the unreacted substances extracted and NC control. The

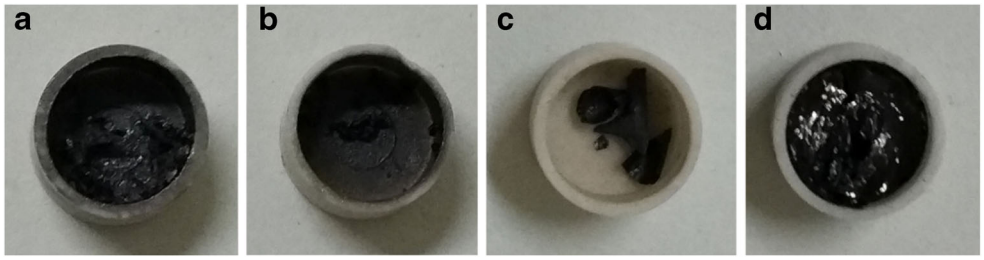

Fig. 5 Digital photographs of the char residues after TGA test for NC control (**a**), 4.5 wt.% T_7-POSS-NC (**b**), 8.6 wt.% T_7-POSS-NC (**c**) and 12.3 wt.% T_7-POSS-NC (**d**)

corresponding data are listed in Table 3. The calculated weight content of Si as determined by the atomic concentrations of the C, N, O and Si elements, indicates that T_7-POSS actively takes part in the cross-linking reaction. Additionally, the calculated weight content of Si increases with the T_7-POSS content, although its degree of increase gradually decreases, which is consistent with the result of the gel content analysis above.

Thermal stability

The thermal stability of NC control and T_7-POSS-NC hybrid materials were evaluated by TGA under a nitrogen atmosphere. The TGA and DTG curves are shown in Fig. 4, and the corresponding data are summarized in Table 4. The $T_{5\%}$ values of 4.5 wt.% T_7-POSS-NC, 8.6 wt.% T_7-POSS-NC and 12.3 wt.% T_7-POSS-NC are decreased slightly compared with that of NC control. As previously reported, the urethane bond is unstable and decomposes at elevated temperature because it will dissociate and re-associate simultaneously from approximately 160 °C [26]. Thus, we suspect that the $T_{5\%}$ values of 4.5 wt.% T_7-POSS-NC, 8.6 wt.% T_7-POSS-NC and 12.3 wt.% T_7-POSS-NC being lower than that of NC control is due to the partial decomposition of the urethane bonds in the T_7-POSS-NC hybrid materials. Although the initial decomposition temperature decreases, the thermal stability of the T_7-POSS-NC hybrid materials is improved significantly in the high temperature region. The $T_{50\%}$ of NC control is 183.3 °C, and the value of 4.5 wt.% T_7-POSS-NC is not significantly different. This result may be explained by the cross-linking density of 4.5 wt.% T_7-POSS-NC not being sufficiently high to form a very tight network, as will be shown in following illustration. The $T_{50\%}$ values of 8.6 wt.% T_7-POSS-NC and 12.3 wt.% T_7-POSS-NC shift to temperatures approximately 25 °C and 60 °C higher, respectively, indicating that the thermal stability of the T_7-POSS-NC hybrid materials at high temperature is improved. Additionally, NC control shows a single and rapid weight loss step with a WLR_{max} value of 432.9%/min, and the char residues are only 1.4% at 500 °C. In the case of 4.5 wt.% T_7-POSS-NC, the WLR_{max} is decreased to 59.5%/min, and the char residues are increased to 9.7% at 500 °C. The WLR_{max} values of 8.6 wt.% T_7-POSS-NC and 12.3 wt.% T_7-POSS-NC are decreased to 1.4%/min and 1.3%/min, respectively, and their char residues are increased to 20.3% and 26.0%, respectively. The increase in the char residue gives rise to the formation of more stable char layers, which may protect the materials from further decomposition and in turn increases the thermal stability [27]. The trend of the TGA results is consistent with the gel content and weight content of Si mentioned above, indicating that the formation of a compact cross-linked network is the key factor for the thermal properties of T_7-POSS-NC hybrid materials [28].

$T_{5\%}$: initial decomposition temperature based on 5% weight loss; $T_{50\%}$: middle decomposition temperature based on 50% weight loss; WLR_{max}: maximum weight loss rate; CR_{500} °C: char residue under 500 °C.

Morphology of char residues

Fig. 5 presents digital photographs of the char residues after the TGA test for each sample. The char residues for NC control and 4.5 wt.% T_7-POSS-NC are sparse, and the black traces on internal surfaces of the two crucibles are caused by the gaseous pyrolysis products that come from the rapid pyrolysis of NC control and 4.5 wt.% T_7-POSS-NC. By contrast, the char residues gradually increased through the formation of a compact cross-linked network and nearly keep their original shape for 8.6 wt.% and 12.3 wt.% T_7-POSS-NC.

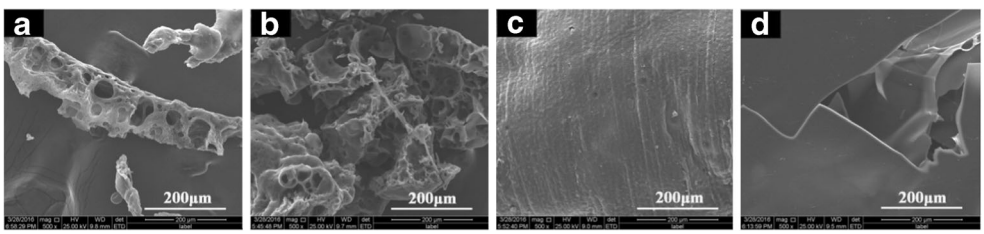

Fig. 6 SEM images of char residues after TGA test for NC control (**a**), 4.5 wt.% T_7-POSS-NC (**b**), 8.6 wt.% T_7-POSS-NC (**c**) and 12.3 wt.% T_7-POSS-NC (**d**)

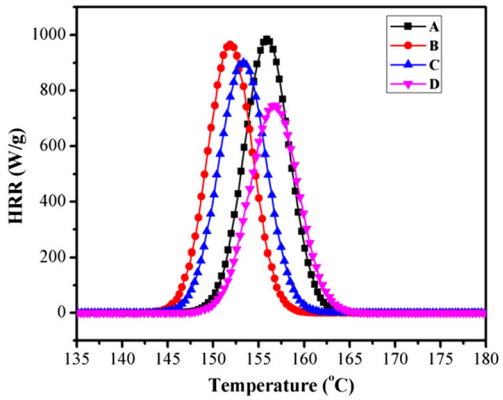

Fig. 7 HRR curves of NC control (**A**), 4.5 wt.% T_7-POSS-NC (**B**), 8.6 wt.% T_7-POSS-NC (**C**) and 12.3 wt.% T_7-POSS-NC (**D**)

To further clarify the morphology of the char residues after the TGA testing, the outer surface of the char residues for all samples was studied by SEM (Fig. 6). The char residues of NC control and 4.5 wt.% T_7-POSS-NC present loose structures with many holes, which make the char layers become fragmented after being heated. By contrast, the char residues of 8.6 wt.% T_7-POSS-NC and 12.3 wt.% T_7-POSS-NC are continuous, with a compact structure on the surface, which is mainly attributed to the formation of a cross-linked network. Additionally, the Si-O-Si structure of the T_7-POSS may provide a stable layer of protection on the NC matrix [29].

Combustion safety

The peak heat release rate (pHRR) of the materials is probably the most important parameter in determining its hazard in a fire [30]. Therefore, MCC was performed to estimate the combustion safety of all samples. Fig. 7 presents the HRR curves of various samples versus temperature. The detailed data obtained from the MCC results, including the pHRR, heat release capacity (HRC) and sum heat release capacity (sHRC), are summarized in Table 5. NC control presents the highest flammability, with a pHRR value of 984.3 W/g, HRC value of 1362 J/g·K and sHRC value of 1241 J/g·K. Incorporating T_7-POSS into the NC sample reduces the pHRR, HRC and sHRC, especially for 12.3 wt.% T_7-POSS-NC, for which they remarkably decrease by 24.1%, 23.6% and 24.9%, respectively, suggesting that the combustion safety of 12.3 wt.% T_7-POSS-NC is clearly improved. Notably, the decreasing trend of the MCC results is not in conformance with that of the gel content efficiency above. This result may be because either the cross-linked network or unreacted T_7-POSS particles contribute to the improvement of the combustion safety.

Table 5 MCC parameters of NC control and T_7-POSS-NC hybrid materials

Samples	pHRR (W/g)	HRC (J/g·K)	sHRC (J/g·K)
NC control	984.3	1362	1241
4.5 wt.% T_7-POSS-NC	965.2	1322	1200
8.6 wt.% T_7-POSS-NC	901.6	1267	1150
12.3 wt.% T_7-POSS-NC	746.9	1041	932

Mechanical properties

Fig. 8 presents the stress-strain curves, tensile strengths and tensile moduli of all samples. The related data are shown in Table 6. Both 4.5 wt.% T_7-POSS-NC and 8.6 wt.% T_7-POSS-NC exhibit higher tensile strengths than that of NC control, which is attributed to the formation of cross-linking networks among NC, T_7-POSS and IPDI. It is noteworthy that the tensile strength of 12.3 wt.% T_7-POSS-NC is decreased, whereas its elongation at break is drastically increased from 3.84% for NC control to 8.78%. As we know, T_7-POSS acts both as a cross-linking agent and as a plasticizing agent in the polymer matrix [22]. When the content of T_7-POSS is low, cross-linking plays the leading role; by contrast, when the content is high, the plasticization of nanoparticles occupies the dominant position. In other words, the two main factors are in a competition state. On the one hand, restraining the fracture of materials depends on restricting the polymer chain slippage on relatively large spatial scales [31] because of the cross-linking, which is the main reason for the improvement of the tensile strength. On the other hand, the blended T_7-POSS nanoparticles increase the free volume [31], which enhances the ductility and reduces the rigidity of the T_7-POSS-NC hybrid materials. Intuitively, the elongation at break increases but the tensile modulus decreases. In addition, the introduction of T_7-POSS weakens the interactions (e.g., hydrogen bonding) between NC molecules in the T_7-POSS-NC hybrid materials, which is also the reason for the decrease in the tensile moduli of the T_7-POSS-NC hybrid materials.

Figure 9 can be used to visually explain the mechanical results mentioned above. As depicted, the NC control (Fig. 9a) is a linear polymer, whereas the T_7-POSS-NC hybrid materials present cross-linking networks. Moreover, the cross-linking degree of the T_7-POSS-NC hybrid materials is proportional to the T_7-POSS content to some extent. For example, when 4.5 wt.% and 8.6 wt.% T_7-POSS are incorporated into the NC, the

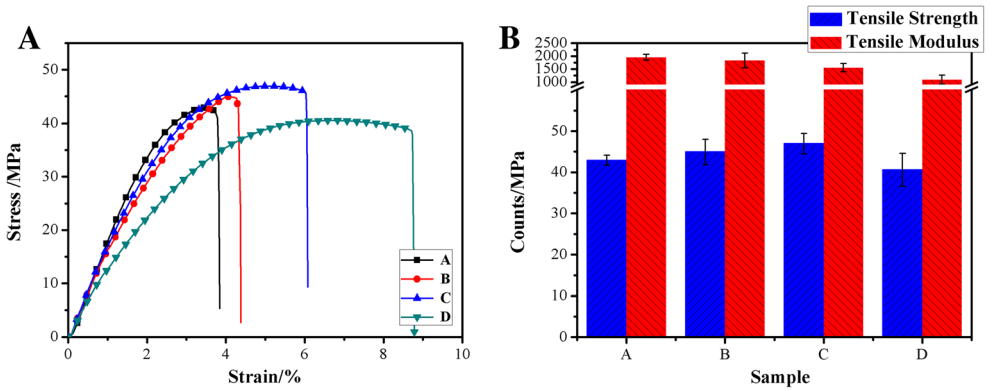

Fig. 8 Stress-strain curves (**a**), tensile strengths and tensile moduli results (**b**) of NC control (**A**), 4.5 wt.% T_7-POSS-NC (**B**), 8.6 wt.% T_7-POSS-NC (**C**) and 12.3 wt.% T_7-POSS-NC (**D**)

Table 6 Mechanical properties of NC control and T_7-POSS-NC hybrid materials

Samples	Tensile strength (MPa)	Elongation at break (%)	Tensile modulus (MPa)
NC control	42.9 ± 1.2	3.84 ± 0.32	1953 ± 108
4.5 wt.% T_7-POSS-NC	44.9 ± 3.1	4.37 ± 0.76	1828 ± 281
8.6 wt.% T_7-POSS-NC	46.9 ± 2.5	6.08 ± 0.91	1553 ± 156
12.3 wt.% T_7-POSS-NC	40.6 ± 4.0	8.78 ± 0.87	1084 ± 174

degree of cross-linking is increased gradually (Fig. 9b, c). In this case, the cross-linking factor in the competition dominates, which gradually increases the tensile strength of the NC hybrid materials. When 12.3 wt.% T_7-POSS is introduced into the NC (Fig. 9d), the cross-linking degree may become saturated, and the unreacted (blended) T_7-POSS nanoparticles, acting as plasticizers, effectively increase the elongation at break. As we know, the material brittleness is inversely proportional to the elongation at break [32]. Therefore, the plasticization of T_7-POSS can be a solution for the ductility improvement and the brittleness reduction of NC-based materials.

Distribution of T_7-POSS

The thermal and mechanical properties of the resultant hybrid materials are affected by the distribution of the POSS moieties in the polymer matrices. The morphologies of the fractured surfaces for all samples as determined by SEM are shown in Fig. 10. T_7-POSS with a dimension of approximately 2 μm is well distributed in the entire region according to the SEM and EDS Si maps, leading to improved thermal and mechanical properties of the T_7-POSS-NC hybrid materials. The weight percentage of Si of the fracture surface for 4.5 wt.% T_7-POSS-NC, 8.6 wt.% T_7-POSS-NC and 12.3 wt.% T_7-POSS-NC as detected by the EDS Si maps is 0.91%, 1.71% and 1.94%, respectively, and the increasing trend coincide with the results of the XPS. It is noteworthy that 12.3 wt.% T_7-POSS-NC shows a coarse fractured surface and plastic flow property, which is very different from 4.5 wt.% T_7-POSS-NC and 8.6 wt.% T_7-POSS-NC. This phenomenon can further confirm that the increasing of the elongation at break mentioned above is related to the

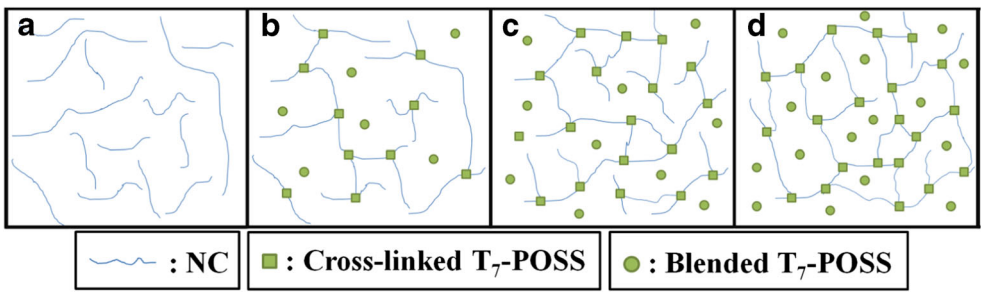

Fig. 9 Illustration of NC control (**a**), 4.5 wt.% T_7-POSS-NC (**b**), 8.6 wt.% T_7-POSS-NC (**c**) and 12.3 wt.% T_7-POSS-NC (**d**)

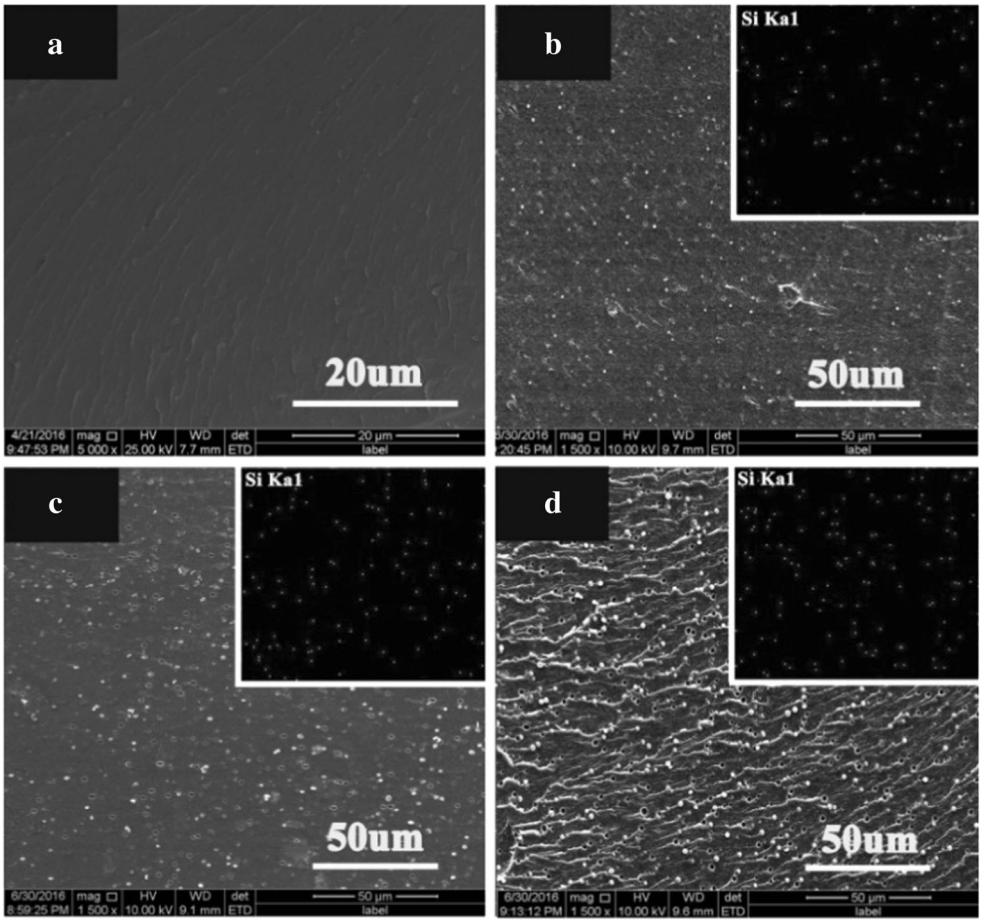

Fig. 10 SEM image of fracture surface for NC control (**a**), 4.5 wt.% T_7-POSS-NC (**b**), 8.6 wt.% T_7-POSS-NC (**c**) and 12.3 wt.% T_7-POSS-NC (**d**)

unreacted T_7-POSS nanoparticles that act as plasticizers in the T_7-POSS-NC hybrid materials.

Conclusion

Novel T_7-POSS-NC hybrid materials with superior thermal stability, high combustion safety and good mechanical properties have been successfully prepared, and the performances are comprehensively characterized. After extracting the unreacted substance, the gel content of the T_7-POSS-NC hybrid materials increased from 40.6% to 65.5%. When 12.3 wt.% T_7-POSS was incorporated into the NC sample, the $T_{50\%}$ shifted upward by 60.2 °C higher, the WLR_{max} decreased by 99.7%, and the char residues were 18.6 times as heavy as that of NC control based on the TGA results. Meanwhile, the peak heat release rate, the heat release capacity and the sum heat release capacity were remarkably reduced by 24.1%, 23.6%, and 24.9%, respectively. These results clearly indicate the improvement of the thermal stability and combustion safety of T_7-POSS-NC hybrid materials, and the mechanical properties of the T_7-POSS-NC hybrid materials were also improved to some extent. In detail, the tensile strength can be increased from 42.9 MPa to 46.9 MPa, and the elongation at break can be increased from 3.84% to 8.78% after incorporating different contents of T_7-POSS. In summary, the improvement in the thermal stability, combustion safety and mechanical properties for T_7-POSS-NC hybrid materials are attributed to the formation of a cross-linked network, the incorporation of unreacted T_7-POSS particles and the good distribution of T_7-POSS.

Acknowledgements The authors thank the National Natural Science Foundation of China (No. 21474008).

Reference

1. Książczak A, Gołofit T, Tomaszewski W (2008) Binary system nitrocellulose from linters symdiethyldiphenylurea. J Therm Anal Calorim 91:375–380
2. Shukla MK, Hill F (2012) Theoretical investigation of reaction mechanisms of alkaline hydrolysis of 2,3,6-trinitro-β-d-glucopyranose as a monomer of nitrocellulose. Struct Chem 23:1905–1920
3. Książczak A, Ostrowski M (2004) DSC studies on long-term properties of nitrocellulose and SYM-diphenylurea system. J Therm Anal Calorim 77:341–351

4. Rychlý J, Lattuati-Derieux A, Matisová-Rychlá L, Csomorová K, Janigová I, Lavédrine B (2012) Degradation of aged nitrocellulose investigated by thermal analysis and chemiluminescence. J Therm Anal Calorim 107:1267–1276
5. Makashir PS, Mahajan RR, Agrawal JP (1995) Studies on kinetics and mechanism of initial thermal decomposition of nitrocellulose. J Therm Anal Calorim 45:501–509
6. Li R, Xu HM, Hu HL, Yang GC, Wang J, Shen JP (2014) Microstructured Al/Fe_2O_3/nitrocellulose energetic fibers realized by electrospinning. J Energ Mater 32:50–59
7. Xiao ZG, Ying SJ, He WD, Xu FM, Sun P (2007) Synthesis, morphology, component distribution, and mechanical properties of nitrocellulose/gradient poly(ethylene glycol dimethacrylate) semi-IPN material. J Appl Polym Sci 105:510–514
8. de Klerk WPC (2015) Assessment of stability of propellants and safe lifetimes. Propell Explos Pyrot 40:388–393
9. Zhao NN, Li JC, Gong HJ, An T, Zhao FQ, Yang AW, Hu RZ, Ma HX (2016) Effects of α-Fe_2O_3, nanoparticles on the thermal behavior and non-isothermal decomposition kinetics of nitrocellulose. J Anal Appl Pyrol 120:165–173
10. Zhang X, Hikal WM, Zhang Y, Bhattacharia SK, Li L, Panditrao S, Wang SR, Weeks BL (2013) Direct laser initiation and improved thermal stability of nitrocellulose/graphene oxide nanocomposites. Appl Phys Lett 102:141905–1(1–4)
11. Katoh K, Ito S, Ogata Y, Kasamatsu J, Miya H, Yamamoto M, Wada Y (2009) Effect of industrial water components on thermal stability of nitrocellulose. J Therm Anal Calorim 99:159–164
12. Raaijmakers MJT, Kappert EJ, Nijmeijer A, Benes NE (2015) Thermal imidization kinetics of ultrathin films of hybrid poly(POSS-imide)s. Macromolecules 48:3031–3039
13. Joseph AM, Nagendra B, Surendran KP, Gowd EB (2015) Syndiotactic polystyrene/hybrid silica spheres of POSS siloxane composites exhibiting ultralow dielectric constant. Acs Appl Mater Inter 7:19474–19483
14. Neyertz S, Brown D, Raaijmakers MJT, Benes NE (2016) A molecular characterization of hyper-cross-linked hybrid polyPOSS-imide networks. Comp Mater Sci 117:338–353
15. Huang JC, He CB, Xiao Y, Mya KY, Dai J, Siow YP (2003) Polyimide/POSS nanocomposites: interfacial interaction, thermal properties and mechanical properties. Polymer 44:4491–4499
16. Kopesky ET, Mckinley GH, Cohen RE (2006) Toughened poly(methyl methacrylate) nanocomposites by incorporating polyhedral oligomeric silsesquioxanes. Polymer 47:299–309
17. Bershtein V, Fainleib A, Egorova L, Grigoryeva O, Kirilenko D, Konnikov S, Ryzhov V, Starostenko O, Yakushev P, Yagovkina M, Saiter JM (2015) The impact of ultra-low amounts of introduced reactive POSS nanoparticles on structure, dynamics and properties of densely cross-linked cyanate ester resins. Eur Polym J 67:128–142
18. González-Campo A, Núñez R, Viñas C, Boury B (2006) Synthetic approaches to the preparation of hybrid network materials incorporating carborane clusters. New J Chem 30:546–553
19. Clough RL (2001) High-energy radiation and polymers: a review of commercial processes and emerging applications. Nucl Instrum Meth A 185:8–33
20. Cheng JJ, Pan Y, Zhu JT, Li ZZ, Pan JA, Ma ZS (2014) Hybrid network CuS monolith cathode materials synthesized via facile in situ, melt-diffusion for Li-ion batteries. J Power Sources 257:192–197
21. Wang L, Zheng S (2012) Surface morphology and dewettability of self-organized thermosets involving epoxy and POSS-capped poly(ethylene oxide) telechelics. Mater Chem Phys 136:744–754
22. Yin G, Zhang L, Li Q (2016) Preparation and characterization of POSS-cross-linked PCL based hybrid materials. J Polym Res 23:1–11
23. Zhang Y, Mao Y, Chen D, Wu WB, Yi SP, Mo SB, Huang C (2013) Synthesis and characterization of addition-type silicone rubbers (ASR) using a novel cross linking agent PH prepared by vinyl-POSS and PMHS. Polym Degrad Stabil 98:916–925
24. Xiang K, He L, Li Y, Xu C, Li S (2015) Dendritic AIE-active luminogens with a POSS core: synthesis, characterization, and application as chemosensors. RSC Adv 5:97224–97230
25. Vahabi H, Ferry L, Longuet C, Otazaghine B, Negrell-Guirao C, David G, Lopez-Cuesta JM (2012) Combination effect of polyhedral oligomeric silsesquioxane (POSS) and a phosphorus modified PMMA, flammability and thermal stability properties. Mater Chem Phys 136:762–770
26. Hablot E, Zheng D, Bouquey M, Avérous L (2008) Polyurethanes based on castor oil: kinetics, chemical, mechanical and thermal properties. Macromol Mater Eng 293:922–929
27. Jiang SH, Yang HY, Qian XD, Shi YQ, Zhou KQ, Xu HY, Shan XY, Lo SM, Hu Y, Gui Z (2014) A novel transparent cross-linked poly (methyl methacrylate)-based copolymer with enhanced mechanical, thermal, and flame-retardant properties. Ind Eng Chem Res 53:3880–3887
28. Baimark Y (2012) Morphology and thermal stability of cross-linked silk fibroin microparticles prepared by the water-in-oil emulsion solvent diffusion method. Asia Pac J Chem Eng 7:112–117
29. Teo JKH, Teo KC, Pan B, Xiao Y, Lu XH (2007) Epoxy/polyhedral oligomeric silsesquioxane (POSS) hybrid networks cured with an anhydride: cure kinetics and thermal properties. Polymer 48:5671–5680
30. Yang H, Yang CQ, He QL (2009) The bonding of a hydroxy-functional organophosphorus oligomer to nylon fabric using the formaldehyde derivatives of urea and melamine as the bonding agents. Polym Degrad Stabil 94:1023–1031
31. Fan H, Yang R (2013) Flame-retardant polyimide cross-linked with polyhedral oligomeric octa(aminophenyl)silsesquioxane. Ind Eng Chem Res 52:2493–2500
32. Fernández MD, Fernández MJ, Cobos M (2016) Effect of polyhedral oligomeric silsesquioxane (POSS) derivative on the morphology, thermal, mechanical and surface properties of poly(lactic acid)-based nanocomposites. J Mater Sci 51(7):3628–3642